Optics and Spectroscopy, 2024, Vol. 132, No. 2

16

X-ray surface guided modes on a boundary between two different periodical multilayer structures

© *I.R. Prudnikov* [1,2,*], *N.N. Usmanov* [1]

[1] Department of Physics, Moscow State University,
119991 Moscow, Russia
[2] National Research Nuclear University „MEPhI",
115409 Moscow, Russia
[*] e-mail: prudnik@phys.msu.ru

Received March 29, 2023
Revised December 03, 2023
Accepted December 09, 2023

On the basis of an analytical approach and with the help of numerical simulations, it is shown that the excitation of an X-ray surface guided mode is possible under certain conditions on a boundary between two different periodical multilayer structures (multilayer mirrors). This mode propagates along the boundary between the two structures and its intensity decreases exponentially with increasing the distance from a boundary surface deep into each of them. An indication of the appearance of the guided wave is a resonant dip in an X-ray specular reflectivity curve from a set of the two periodical multilayer mirrors that are placed consecutively, one after another, on a substrate. An influence of the thicknesses of films, forming one bilayer, and layer materials in the multilayer structures on peculiarities of a surface wave excitation is investigated.

Keywords: periodical multilayer structure, interface, X-ray surface guided mode, Bragg reflection.

DOI: 10.61011/EOS.2024.02.58452.4765-23

1. Introduction

The existence of the surface electromagnetic waves follows from the solution to the Maxwell equations [1]. Such a wave propagates along the surface (interface) between the two media, and the wave amplitude exponentially decays normally to the surface into the depth of both media. The above wave may be excited if certain requirements are met, which must be met, for example, by the dielectric permittivity values of the bordering materials [1]. The surface optical modes may experimentally be excited between a metal diffraction grating or metal film and a dielectric (air) [1]. These modes are surface plasmons, and the minima appearing during generation of the similar plasmons in the curves of the specular reflection in case of diffraction gratings are known as „Wood's anomalies" [2]. Note that in the monograph [3] the surface electromagnetic waves are treated as a special example of a guided mode, which in general is a traveling wave localized in the plane perpendicular to the direction of its propagation. Along with the border between the homogeneous media, the localized optical electromagnetic waves may exist also on the surface of a photonic-crystal structure with the periodical variation of the refraction index, for example, on the border of photonic crystal/air [4], photonic crystal/metal film [5], photonic crystal/photonic crystal [6].

For electromagnetic radiation of X-ray range (wavelength $\sim 1\,Å$) the experiments use waveguides, where the guided modes appear as a result of total external reflection of X-rays at the interface between two homogeneous media (two homogeneous films) with the grazing angles of incidence near the critical angle of total external reflection [7–13]. In contrast to [7–13] the papers [14–16] analyze the possibility of exciting the X-ray waveguide modes with the help of Bragg reflections from the periodical multilayer structures [14,15] and crystalline films [16]. Theoretical and experimental research of the localized X-ray modes on the surface of crystals under the diffraction conditions at grazing angles of incidence was conducted in [17,18]. It follows from the results of analytical calculations and numerical simulation that the X-ray surface waves may exist also on the border between the periodical multilayer structure and the film [19] or air [20] and on the interface of the crystalline superlattice and the crystal film [21,22].

Note that recently the papers have been appearing with the results of new experiments and/or ideas of new experiments in the field of the quantum X-ray optics [23,24] and nuclear resonance scattering [24,25] using X-ray waveguides (for detailed review of the corresponding topic see references in [24,25]). For example, in [23] it is shown that placement of a thin film (film thickness 2.8 nm) of tungsten disilicide WSi_2 into a waveguide may, with the help of the excitation of the X-ray guided mode, vary (reduce) the lifetime of the tungsten atom excited state in a controlled manner. Such a state arises as a result of electron removal (ionization) from one of the internal shells of the atom that are located closely to the nucleus. The authors [23] emphasize that in the experiment such a control is important in research of dynamics of ultrafast processes that are possible using X-ray free-electron lasers.

From the recent papers dedicated to X-ray waveguides, we would also like to highlight the article [13], where the X-ray waveguide served as a source of both the characteristic X-ray radiation and the X-ray radiation of continuous spectrum. In the experiment the electron beam bombarded the thin (thickness 1–2 nm) metal film placed into a guiding layer. Intensity of the X-ray emission released as a result of exposure to the electron beam increased as a result of guided mode excitation. In opinion of the authors [13], the conducted experiments open the door to development of laboratory sources of X-ray radiation with high intensity.

Recently the search continues for the new combinations of materials, which will make it possible to obtain the highest intensity of the X-ray guided mode in the experiment. Thus, paper [26] experimentally researched the triple layer Ru/C/Ru, and its optimal structural parameters are determined, which are necessary to generate a guided mode with the maximum intensity in the carbon layer.

This paper shows that the localized X-ray wave or X-ray surface guided mode (according to the definition [3]) may be excited on the border surface between the two different periodical multilayer structures. The considered problem is formally similar to the task on the surface electromagnetic states at the border of photonic crystal/photonic crystal [6]. The article formulates the conditions necessary for effective generation of such a wave in the experiment.

2. Analytical method

Let us consider specular reflection of X-rays in a specimen consisting of two various periodical multilayer structures (Fig. 1). The first multilayer structure (MS1) is located directly on the second one (MS2). The interface MS1/air, at grazing angle ϑ, is hit with a planeσ-polarized wave with frequency ω and amplitude E_0. Let us find the expression for the wave electric field at the interface between MS1 and MS2 (Fig. 1). For the calculations we shall assume that MS1 and MS2 are divided by the imaginary infinitely thin vacuum gap with thickness l_Δ. The wave electric field that depends on coordinate z inside the gap can be represented in the form of

$$E(z) = E_t \exp[ik_\Delta(z - l - l_\Delta)] + E_r \exp[-ik_\Delta(z - l - l_\Delta)], \quad (1)$$

where l — thickness of MS1, so that equation $z = l$ determines the interface MS1/MS2(Fig. 1), E_t and E_r — amplitudes of transmitted (index „t“) and reflected (index „r“) waves inside the vacuum gap, $\pm k_\Delta$ — projections of the wave vectors of the specified waves on the axis z, coordinate z changes inside the vacuum gap, $l \le z \le l + l_\Delta$. In (1) we omitted the phase factor $\exp(ik_0\cos(\vartheta)x - i\omega t)$,

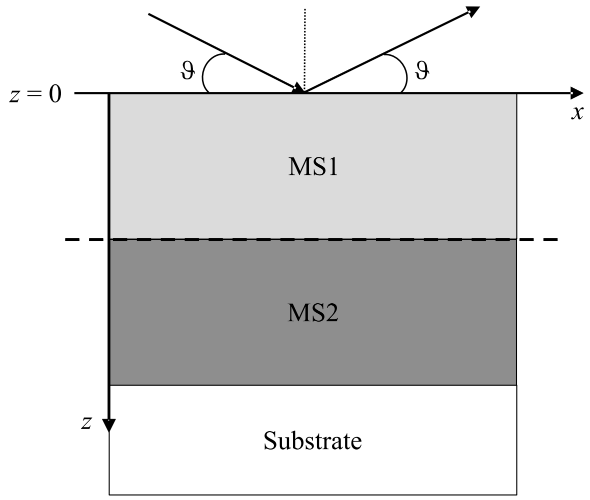

Figure 1. The illustrative view of the multilayer structure comprising two periodical multilayer structures MS1 and MS2; MS2 is located on the substrate; MS1 is located directly on MS2. The horizontal dashed line shows the interface between MS1 and MS2, where the X-ray surface guided mode appears that propagates along this interface. The surface mode is excited with the help of an X-ray wave incident on the incoming surface of the specimen, $z = 0$, at grazing angle ϑ; the specular reflection of the specified X-ray wave from the entire multilayer structure made of MS1 and MS2, happens in the plane xz.

which determines the dependence on time and longitudinal coordinate x (Fig. 1), where $k_0 = \omega/c$. Based on the approach used in [14], the following equations may be obtained for amplitudes E_r and E_t:

$$E_t \exp(-ik_\Delta l_\Delta) = T_1 E_0 + \bar{R}_1 E_r \exp(ik_\Delta l_\Delta), \ \text{at } z = l,$$

$$E_r = R_2 E_t, \quad \text{at} \quad z = l + l_\Delta, \quad (2)$$

where T_1 and $\bar{R}_1$ — complex amplitude coefficients of transmission and specular reflection for MS1, the line above the coefficient $\bar{R}_1$ means that this coefficient describes the specular reflection from MS1, when the wave falls from the vacuum gap to the interface $z = l$, the transmission coefficient T_1 determines the amplitude of the wave that passes through MS1 into the vacuum gap, at $z = l$, R_2 — the complex amplitude coefficient of specular reflection from MS2 at the interface $z = l + l_\Delta$. Using equations (2) we find the expressions for the amplitudes E_t and E_r:

$$E_t = T_1 \exp(ik_\Delta l_\Delta) E_0/[1 - \bar{R}_1 R_2 \exp(i2k_\Delta l_\Delta)],$$

$$E_r = T_1 R_2 \exp(ik_\Delta l_\Delta) E_0/[1 - \bar{R}_1 R_2 \exp(i2k_\Delta l_\Delta)]. \quad (3)$$

Assuming the thickness l_Δ in (1) and (3) as equal to zero, $l_\Delta = 0$, from (1) and (3) we find the expression for the field at $z = l$:

$$E(z = l) = \frac{T_1(1 + R_2)}{(1 - R_1 R_2)} E_0. \quad (4)$$

Since the condition of continuity of the tangential component of the electric field strength vector should be met upon transition from the vacuum gap in MS1 and MS2, the expression (4) determines the value of the electric field at the interface of MS1/MS2 at $z = l$.

Let us record the product $\bar{R}_1R_2$ in the denominator of the formula (4) as $\bar{R}_1R_2 = |\bar{R}_1||R_2|\exp(i\varphi)$, where φ — phase of the product of coefficients $\bar{R}_1R_2$. Let the main value φ be within the interval of $-\pi < \varphi \leq \pi$. When the condition is met,

$$\varphi(\vartheta) = 0, \quad (5)$$

then the denominator in (4) has the form of $1 - |\bar{R}_1||R_2|$. In case of dynamic diffraction of the X-Rays simultaneously in MS1 and MS2, the product $|\bar{R}_1||R_2| \sim 1$ and the difference $1 - |\bar{R}_1||R_2|$ tends to vanish, which causes increase of the field amplitude $|E(z = l)|$ at the interface of MS1/MS2. Therefore, if in the certain interval of the grazing angles the areas of the strong Bragg reflection from MS1 and MS2 overlap, and in this interval at a certain grazing angle the condition (5) is met, then at the specified angle the amplitude of the wave field (4) at the interface of MS1/MS2 increases resonantly. As it moves away from the border of $z = l$ into the depth of MS1 or MS2 the amplitude of the wave field exponentially decreases because of the primary extinction phenomenon as a result of the dynamic diffraction of X-rays in the periodical multilayer structures and perfect crystals [27,28]. In section 4 there are numerical examples, which illustrate the above listed features of the resonance increase of the wave field amplitude for different periodical multilayer structures.

3. A Method to calculate the curve of specular reflection and intensity of the wave field inside the multilayer structure

All numerical results in the article are obtained on the basis of the Parratt recurrence relations [29]. The papers [30–32] specify the methods to calculate the intensity of the wave reflected specularly from or that passed through the rough interface between the two media, which are true for the arbitrary value of the mean square amplitude of roughness of that interface and also take into account the longitudinal length of correlation (correlation function of the random roughness) [30,32]. However, even in case of one interface within these methods it is necessary to numerically solve the integral Fredholm equation of the first kind [30,32], which requires the special mathematical algorithms and, as a result, a significant time of computer calculations. For this reason in this paper for the computer simulation of all theoretical curves of specular reflection from the multilayer structure and the distribution of the wave field in the depth of such a structure, the approximated approach is applied, which is often used in the literature [33]: influence of interlayer roughnesses is taken into account with the help of multiplying the reflection (Fresnel) and transmission coefficients for each interface between the layers by the corresponding corrective factors as it is proposed in the widely known papers [34,35]. After the specified changes, the reflection and transmission coefficients are substituted into the Parratt recurrence relations [29].

4. Results of numerical simulation and discussion of the obtained results

Let us consider the structure

$$\mathrm{Si(substrate)}/\underbrace{20 \times [\mathrm{Ni}(5\,\mathrm{nm})/\mathrm{C}(5\,\mathrm{nm})]}_{\mathrm{MS2}}/\underbrace{14 \times [\mathrm{Ni}(1.5\,\mathrm{nm})/\mathrm{C}(8\,\mathrm{nm})]}_{\mathrm{MS1}}/\mathrm{air}, \quad (6)$$

where numbers 20 and 14 — the number of bilayers Ni/C for MS2 and MS1, accordingly, the round brackets contain (average) thicknesses of the nickel and carbon layers. The mean square amplitude of roughness, σ, is equal to 0.5 nm for all the interfaces inside MS1 and MS2 for the structure (6) and other subsequent structures considered in this article. Densities of nickel and carbon: $\rho_{\mathrm{Ni}} = 8.9\,\mathrm{g/cm^3}$ and $\rho_{\mathrm{C}} = 2.0\,\mathrm{g/cm^3}$. If the wavelength of X-rays incident on (6) is equal to $\lambda = 0.154056\,\mathrm{nm}$, then in case of the first Bragg maximum the Bragg angle for MS1 is equal to $\vartheta_1 = 0.5277^\circ$ and for MS2 it is equal to $\vartheta_2 = 0.5469^\circ$. The multilayer structure 1 is characterized by strong Bragg reflection for angles $0.5097^\circ \leq \vartheta \leq 0.5410^\circ$, MS2 — for angles $0.5092^\circ \leq \vartheta \leq 0.5743^\circ$. The area of strong Bragg reflection, or the area of dynamic diffraction of X-rays, is the range of grazing angles, within the limits of which the intensity of the specularly reflected X-ray wave is equal to one for the half-infinite periodical multilayer structure with quite a large number of bilayers, under the idealized condition of the negligibly low absorption of X-rays [28]. In this paper the borders of the area of dynamic diffraction for MS1 and MS2 are determined by the method of numerical simulation. As this takes place, the absorption coefficients in the layers and the mean square amplitudes of roughnesses of the interfaces inside MS1 and MS2 are purely formally assumed to be equal to zero, and the intensity of the reflected wave upon increase of the number of bilayers tends in the limit to one with account of the specified accuracy of the calculations. All other numerical results presented in the paper are obtained already with account of absorption in bilayers Ni/C and the roughnesses of the interfaces.

Fig. 2 shows the change of phase φ near Bragg angles ϑ_1 and ϑ_2. From the figure it follows that at angle $\vartheta = 0.5115^\circ$ the condition (5) is met. The value $\vartheta = 0.5115^\circ$ is in the angular range, where the dynamic diffraction happens simultaneously in MS1 and MS2. Fig. 3, *a* shows the curve of specular reflection of X-rays from the structure (6) in the vicinity of angles ϑ_1 and ϑ_2. At $\vartheta = 0.5115^\circ$, when the

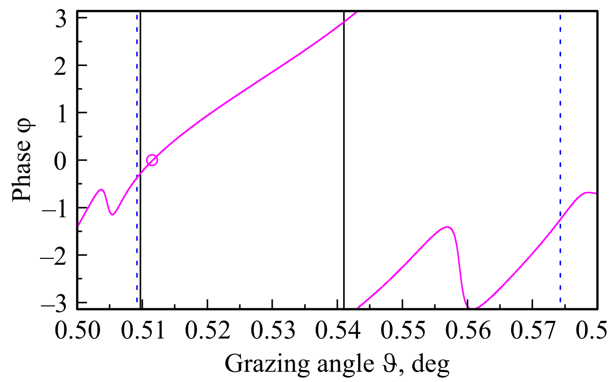

Figure 2. Dependence of phase φ of the product of coefficients $\bar{R}_1 R_2$ on the grazing angle ϑ (see the main text for explanations). Solid vertical lines and dashed vertical lines designate the borders of the area of strong Bragg reflection for MS1 and MS2, respectively, in the case of the first Bragg maximum. The circle on the curve means the point complying with the angle $\vartheta = 0.5115°$. At this angle, the equality $\varphi(\vartheta) = 0$ (5) is met.

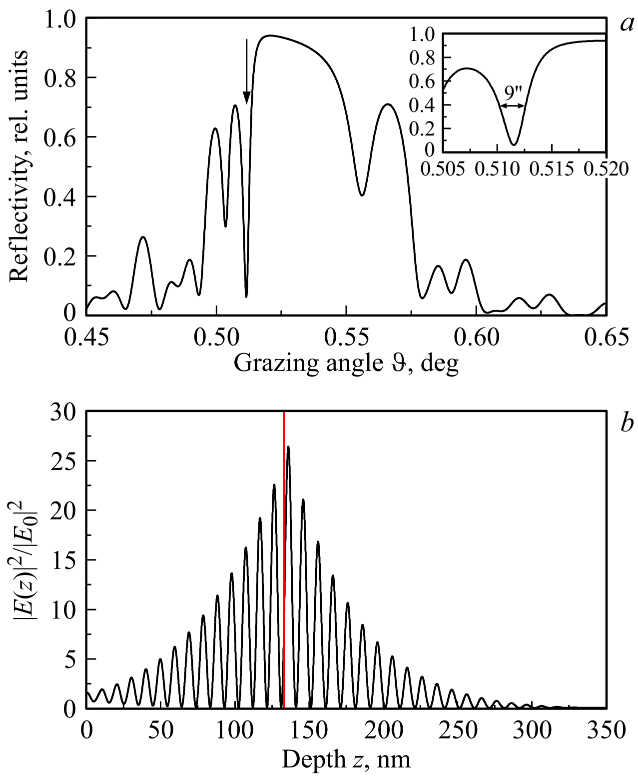

Figure 3. (a) The curve of the specular reflection of X-rays from the structure (6). The vertical arrow indicates the resonance minimum at the angle $\vartheta = 0.5115°$ (Fig. 2). This dip appears as a result of excitation of the surface guided mode at the interface MS1/MS2 inside (6). At the insert to the figure one can see the specified minimum on an enlarged scale. Similarly to Fig. 3, a, the vertical arrow in Fig. 4, a, 5, a, 6, a and 7 indicates the position of the resonance minimum in other curves of specular reflection; at the inserts to Fig. 4, a, 5, a, 6, a and 7 the resonance dip is represented on an enlarged scale. (b) The dependence of the normalized square of the module of the total wave field, $|E(z)|^2/|E_0|^2$ on coordinate z inside (6) under the conditions of excitation of the surface guided mode at fixed angle $\vartheta = 0.5115°$ (a). The vertical line indicates the interface between MS1 and MS2 (the vertical line in Fig. 4, b, 5, b and 6, b also indicates the interface between MS1 and MS2).

condition (5) is met, in this curve there is a deep resonance minimum, which confirms the excitation of the surface guided mode near the interface MS1/MS2. Fig. 3, b shows the distribution of the normalized square of the module, $|E(z)|^2/|E_0|^2$, inside (6), where $E(z)$ — is the sum of two wave (electric) fields: the field of the transmitted wave, which propagates towards the substrate, and the field of the specularly reflected wave (for example, the expression for $E(z)$ is determined by the formula (1) inside the vacuum gap with thickness l_Δ). Both the fields depend on the coordinate z (Fig. 1). Near the interface $z = l$ between MS1 and MS2 the above distribution has the maximum related to the excitation of the surface guided mode. With distance from the interface $z = l$ the envelope of the distribution $|E(z)|^2/|E_0|^2$ exponentially decays both in depth of MS1 and in depth of MS2 due to the phenomenon of the primary extinction at dynamic diffraction of X-rays in the periodic media [27,28]. For this reason the guided mode propagates along the interface $z = l$. Note that from Fig. 3, b it follows that all maxima for $|E(z)|^2$ are in the carbon layers. One can consider, that upon appearance of the surface guided mode in MS1 and MS2, the Borrmann mode of the interference X-ray field is excited, which complies with the weak absorption of the wave upon dynamic diffraction in the periodical medium [27,28]. The guided mode also appears, if in contrast to (6) MS2 with the bilayer C(8 nm)/Ni(1.5 nm) is located on the substrate, and directly above it there is MS1 with the bilayer C(5 nm)/Ni(5 nm):

$$\mathrm{Si(substrate)}/30 \times [\mathrm{C(8\,nm)/Ni(1.5\,nm)}]/$$
$$7 \times [\mathrm{C(5\,nm)/Ni(5\,nm)}]/\mathrm{air}. \qquad (7)$$

The structure (7) is inverted compared to (6). Fig. 4 shows the curve of the specular reflection and dependence of the normalized square of the module $|E(z)|^2/|E_0|^2$ on the coordinate z for (7). The maximum value for $|E(z)|^2/|E_0|^2$ is located near the interface between MS1 and MS2 and is numerically equal to ~ 26 (Fig. 3, b) and ~ 28 (Fig. 4, b).

The guided mode may be excited also in the case when inside MS1 or MS2 (Fig. 1) the thickness of the nickel films is much larger than the thickness of the carbon films. Let us turn, for example, to the following structure (for comparison, see (6)):

$$\mathrm{Si(substrate)}/20 \times [\mathrm{C(5\,nm)/Ni(5\,nm)}]/$$
$$5 \times [\mathrm{C(1.5\,nm)/Ni(11\,nm)}]/\mathrm{air}. \qquad (8)$$

Fig. 5, b shows that in contrast with (6) and (7) for (8) the maxima $|E(z)|^2$ are in the carbon layers only inside MS2 (Borrmann mode of the field), and in MS1 they are located in the Ni films near the interface C/Ni (anti-

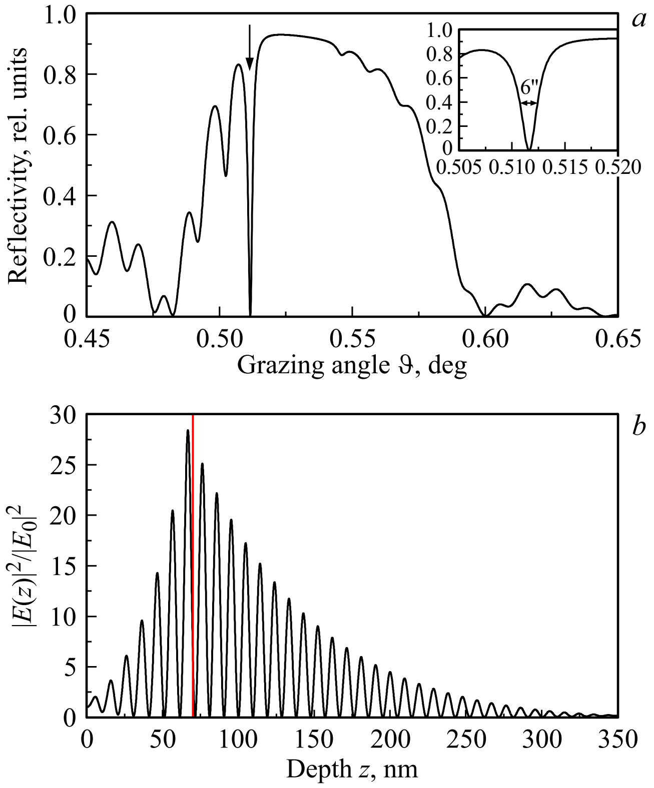

Figure 4. (*a*) The curve of the specular reflection of X-rays from the structure (7), which is inverted compared to (6). The resonance minimum is located at $\vartheta = 0.5116°$. (*b*) Distribution of the normalized square of the module of the total wave field inside (7) at $\vartheta = 0.5116°$.

Borrmann mode of the field). For this reason the maximum value of distribution $|E(z)|^2/|E_0|^2$ in the vicinity of the interface MS1/MS2 is equal to ~ 9 and is less than 26 (Fig. 3, *b*) and 28 (Fig. 4, *b*). As a result of the specified features, for (8) the angular half-width of the resonance minimum $\sim 16''$ (Fig. 5, *a*) and is larger than those values that are specified on the inserts to Fig. 3, *b* and 4, *b*.

If the thicknesses of the Ni and C films are reduced, for example, to the following values (compare with (6) and (7)):

$$\mathrm{Si(substrate)}/30 \times [\mathrm{C(4.5\,nm)/Ni(1.5\,nm)}]/$$
$$30 \times [\mathrm{C(3\,nm)/Ni(3\,nm)}]/\mathrm{air}, \qquad (9)$$

then Bragg angles will become equal to $\vartheta_1 = 0.8030°$ and $\vartheta_2 = 0.7845°$. The condition (5) for (9) is met at angle $\vartheta = 0.7755°$, which is not in the range, where the areas of strong Bragg reflections from MS1 and MS2 overlap. Fig. 6, *a* demonstrates that at $\vartheta = 0.7755°$ there is a deep resonance minimum in the curve of the specular reflection. However, the envelope of distribution $|E(z)|^2/|E_0|^2$, complying with the specified fixed angle, exponentially decays only inside MS2, and inside MS1 this envelope has the maximum (Fig. 6, *b*). This feature is due to the fact that the value $\vartheta = 0.7755°$ is inside the area of strong diffraction reflection for MS2 and is outside this area in case of MS1. We assume that dependence $|E(z)|^2$, shown in Fig. 6, *b*, complies with the surface quasi-guided mode.

Nickel and carbon in structures MS1 and MS2 (Fig. 1) may be replaced with other materials. In doing so, for excitation of the surface mode it is still necessary to comply with the condition (5), which was discussed above. For example, Fig. 7 shows the curve of specular reflection, which complies with the structure (6), if in (6) the Ni(1.5 nm) films are replaced with Mo(1.5 nm) films with density $\rho_{\mathrm{Mo}} = 10.22\,\mathrm{g/cm^3}$ (for comparison see Fig. 3, *a*).

5. Conclusion

From the results of the analytical consideration and numerical calculations it follows that at the interface between two different periodical multilayer structures it is possible to excite an X-ray surface guided mode, which propagates along this interface. The amplitude of the mode exponentially decays normally to the surface inside both structures. The paper formulates and discusses the requirements, under which, if they are met, the surface mode appears: the grazing angle determined from equality (5) must be in the angular range, where the areas of strong Bragg reflection

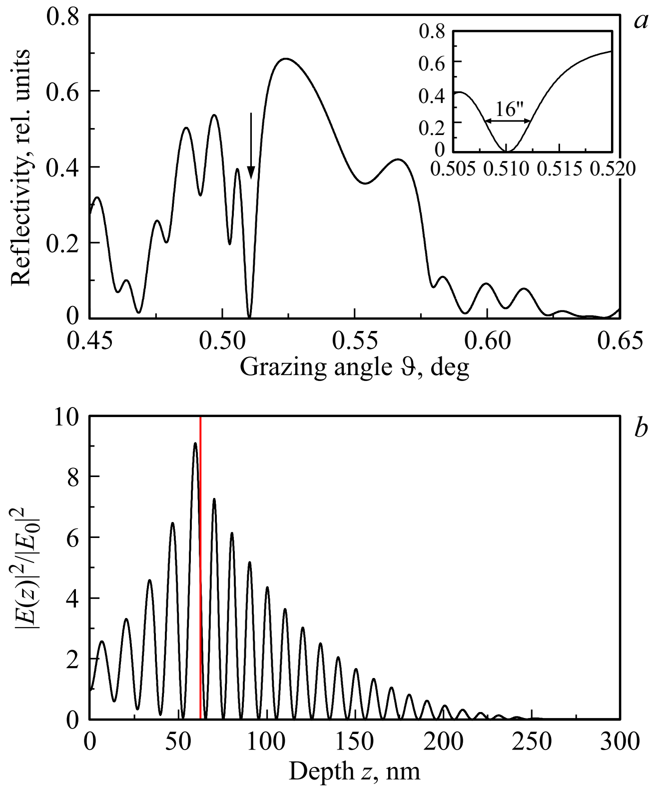

Figure 5. (*a*) The curve of the specular reflection of X-rays from the structure (8), when in MS1 the thickness of nickel films is much larger than the thickness of the carbon films. The resonance minimum is at $\vartheta = 0.5101°$. (*b*) Distribution of the normalized square of the total wave field module inside (8) at $\vartheta = 0.5101°$.

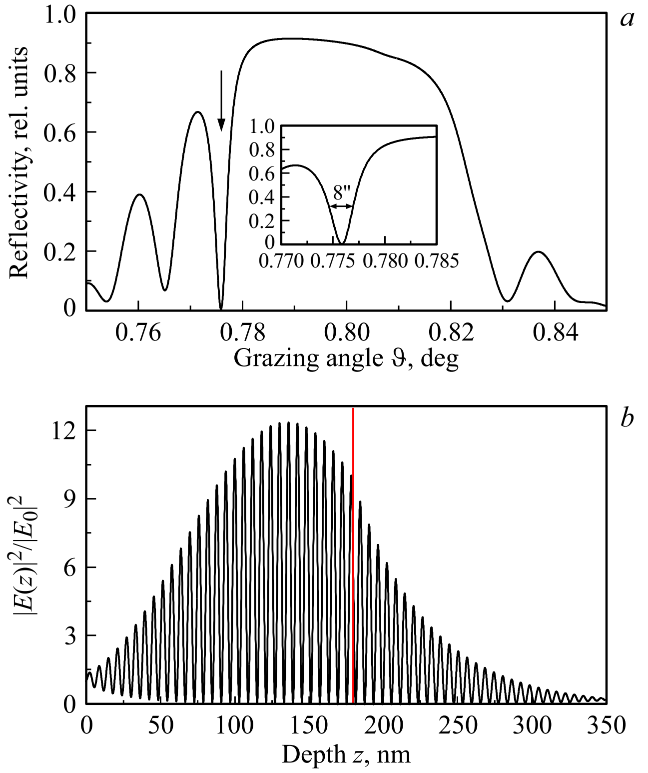

Figure 6. (*a*) The curve of the specular reflection of X-rays from the structure (9). The resonance dip in the curve is in the area of the strong diffraction reflection for MS2 and is located outside this area for MS1. (*b*) Distribution of the normalized square of the module of the total wave field inside (9) upon excitation of the surface quasi-guided mode.

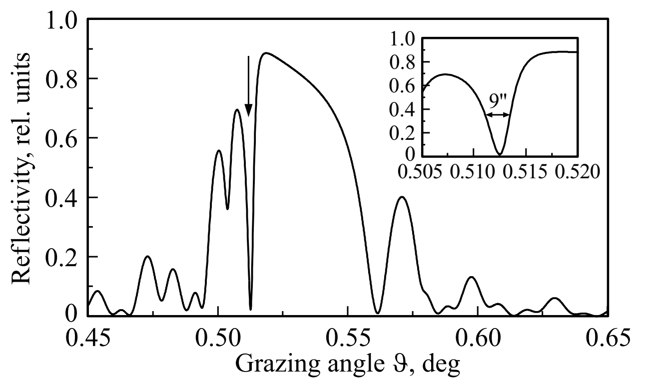

Figure 7. The curve of the specular reflection from the structure (6), where Ni (1.5 nm) films are replaced with Mo (1.5 nm) films.

from two periodically multilayer structures overlap. As illustrated by the multilayer mirrors with bilayers Ni/C it is shown that under certain conditions the appearance of the surface guided mode is accompanied with the excitation of the Borrmann mode of interference X-ray field inside both periodical structures. In this case all maxima of the field are located in the carbon layers with the weak absorption compared to the nickel films. The specified case has the practical value for generation of the surface guided mode in the experiment.

The structure proposed in the paper and composed of two different periodical multilayer mirrors MS1 and MS2, may find the experimental application as an X-ray waveguide together with the waveguides, long used in practice, on the basis of the total external reflection of X-rays near the critical angle of total external reflection. Under certain structural parameters of MS1 and MS2 the maxima of intensity of the interference X-ray field of the waveguide mode, which appears at the interface between MS1 and MS2, are in the layers of the material with the low absorption coefficient. This will result in reduction of absorption of its intensity during propagation inside the waveguide.

The structure analyzed in this paper may also have the potential application as a multilayer anode-waveguide, which is bombarded by the external electron beam. As a result of such an impact at the metal films inside the multilayer structure the X-ray emission may be generated, which is amplified as a result of excitation of the surface guided mode.

Conflict of interest

The authors declare that they have no conflict of interest.

References

[1] H. Raether. *Surface Plasmons on Smooth and Rough Surfaces and on Gratings* (Springer-Verlag, Berlin, 1988). DOI: 10.1007/BFb0048317

[2] R.W. Wood. Philos. Mag., **4** (21), 396 (1902). DOI: 10.1080/14786440209462857

[3] I.R. Shen. *Printsipy nelineinoi optiki*, pod. red. S.A. Akhmanova (Nauka, M., 1989). (in Russian)

[4] W.M. Robertson, M.S. May. Appl. Phys. Lett., **74** (13), 1800 (1999). DOI: 10.1063/1.123090

[5] M. Kaliteevski, I. Iorsh, S. Brand, R.A. Abram, J.M. Chamberlain, A.V. Kavokin, I.A. Shelykh. Phys. Rev. B, **76** (16), 165415 (2007). DOI: 10.1103/PhysRevB.76.165415

[6] A.P. Vinogradov, A.V. Dorofeenko, A.M. Merzlikin, A.A. Lisyansky. Usp. Fiz. Nauk., **180** (3), 249 (2010). DOI: 10.3367/UFNr.0180.201003b.0249.

[7] E. Spiller, A. Segmüller. Appl. Phys. Lett., **24** (2), 60 (1974). DOI: 10.1063/1.1655093

[8] Y.P. Feng, S.K. Sinha, H.W. Deckman, J.B. Hastings, D.P. Siddons. Phys. Rev. Lett., **71** (4), 537 (1993). DOI: 10.1103/PhysRevLett.71.537

[9] S.I. Zheludeva, M.V. Kovalchuk, N.N. Novikova, A.N. Sosphenov, N. E. Malysheva, N.N. Salashchenko, Yu.Ya. Platonov, A.D. Akhsakhalyan. Crystallogr. Rep., **40** (1), 132 (1995).

[10] A.V. Andreev, Yu.V. Ponomarev, I.R. Prudnikov, N.N. Salashchenko. Pis'ma Zh. Éksp. Teor. Fiz., **66** (4), 219 (1997). DOI: 10.1134/1.567460.

[11] V.K. Egorov, E.V. Egorov. Thin Solid Films, **398**, 405 (2001). DOI: 10.1016/S0040-6090(01)01386-4

[12] Q. Zhong, L. Melchior, J. Peng, Q. Huang, Z. Wang, T. Salditt. J. Appl. Cryst., **50** (3), 701 (2017). DOI: 10.1107/S1600576717004630
[13] M. Vassholz, T. Salditt. Sci. Adv., **7** (4), eabd5677 (2021). DOI: 10.1126/sciadv.abd5677
[14] I.R. Prudnikov. J. Appl. Crystallogr., **38** (4), 595 (2005). DOI: 10.1107/S0021889805011830
[15] V.A. Bushuev, O.D. Roshchupkina. Bull. Russ. Acad. Sci. Phys., **72** (2), 192 (2008). DOI: 10.1007/s11954-008-2014-3.
[16] I.R. Prudnikov. Phys. Rev. B, **66** (19), 193309 (2002). DOI: 10.1103/PhysRevB.66.193309
[17] A.V. Andreev. UFN, **145** (1), 113 (1985). [Sov. Phys. Usp., (in Russian) **28** (1), 70 (1985). DOI: 10.1070/PU1985v028n01ABEH003650].
[18] T. Jach, D.B. Novotny, M.J. Bedzyk, Q. Shen. Phys. Rev. B, **40** (8), 5557 (1989). DOI: 10.1103/PhysRevB.40.5557
[19] I.R. Prudnikov. J. Appl. Crystallogr., **39** (2), 259 (2006). DOI: 10.1107/S0021889806003232
[20] A.V. Vinogradov, I.V. Kozhevnikov. JETP Lett., **40** (10), 1221(1984).
[21] I.R. Prudnikov. Acta Crystallogr., Sect. A, **74**(5), 608 (2018). DOI: 10.1107/S2053273318009877
[22] I.R. Prudnikov. J. Struct. Chem. **62** (4), 622 (2021). DOI: 10.1134/S0022476621040144.
[23] X.-C. Huang, X.-J. Kong, T.-J. Li, Z.-R. Ma, H.-C. Wang, G.-C. Liu, Z.-S. Wang, W.-B. Li, L.-F. Zhu. Phys. Rev. Res., **3** (3), 033063 (2021). DOI: 10.1103/PhysRevResearch.3.033063
[24] R. Röhlsberger, J. Evers. In: *Modern Mössbauer Spectroscopy*, ed. by Y. Yoshida, G. Langouche. Topics in Applied Physics (Springer, Singapore, 2021), vol. 137, p. 105–171. DOI: 10.1007/978-981-15-9422-9_3
[25] L. Wolff, J. Evers. Phys. Rev. Res., **5** (1), 013071 (2023). DOI: 10.1103/PhysRevResearch.5.013071
[26] Kiranjot, R. Dhawan, M.H. Modi. Surf Interface Anal., **54** (1), 52 (2022). DOI: 10.1002/sia.7016
[27] Z.G. Pinsker. *Rentgenovskaya kristallooptika*, 2-e izd., pererab. i dop. (Nauka, M. (1982) (in Russian).
[28] A.V. Vinogradov, I.A. Brytov, A.Ya. Grudsky, M.T. Kogan, I.V. Kozhevnikov, V.A. Slemzin. *Zerkalnaya rentgenovskaya optika*, pod. red. A.V. Vinogradova (Mashinostroenie. Leningr. otd-nie, L., 1989). (in Russian)
[29] L.G. Parratt. Phys. Rev., **95** (2), 359 (1954). DOI: 10.1103/PhysRev.95.359
[30] A.V. Andreev. Phys. Lett. A, **219** (5-6), 349 (1996). DOI: 10.1016/0375-9601(96)00469-0
[31] I.D. Feranchuk, S.I. Feranchuk, A.P. Ulyanenkov. Phys. Rev. B, **75** (8), 085414 (2007). DOI: 10.1103/PhysRevB.75.085414
[32] ØS. Hetland, A.A. Maradudin, T. Nordam, P.A. Letnes, I. Simonsen. Phys. Rev. A, **95** (4), 043808 (2017). DOI: 10.1103/PhysRevA.95.043808
[33] M.A. Andreeva, V.A. Bushuev, E.N. Ovchinnikova, A.P. Oreshko, I.R. Prudnikov, A.G. Smekhova. *Chislennye eksperimenty v zadachakh rentgenovskoy optiki*, pod red. A.S. Ilyushina, (MGU im. M.V. Lomonosova, Fizicheskiy fakultet, M., 2005), 149 s. (in Russian)
[34] L. Névot, P. Croce. Rev. Phys. Appl., **15** (3), 761 (1980). DOI: 10.1051/rphysap:01980001503076100
[35] B. Vidal, P. Vincent. Appl. Opt., **23** (11), 1794 (1984). DOI: 10.1364/AO.23.001794

Translated by M.Verenikina